6th International Conference on Advances in Experimental Structural Engineering
11th International Workshop on Advanced Smart Materials and Smart Structures Technology
August 1-2, 2015, University of Illinois, Urbana-Champaign, United States

Experimental study on seismic behavior of composite concrete and double-steel-plate shear walls with binding bars

Chunlan Cheng[1], Deyuan Zhou[2]

1   Institute of Structural Engineering and Disaster Reduction, Tongji University, Shanghai 200092, China.
      E-mail: cclan83@126.com

2   Institute of Structural Engineering and Disaster Reduction, Tongji University, Shanghai 200092, China.
      E-mail: dyzhou@tongji.edu.cn.

ABSTRACT

In order to study the seismic behaviour of composite concrete and steel plate shear walls with binding bars (CCSPW). The cyclic loading tests were conducted on ten specimens of CCSPW. Bolt connection with eight nuts was used between two steel plates. The failure modes, deformation performance and energy dissipation capacity were observed. Valuable results were obtained for the hysteretic loops, bearing capacity, skeleton curves, ductility and energy dissipation capacity. The effects of different aspect ratios, binding bar spacing, plate thicknesses, core concrete thicknesses, axial compression ratios and setting of end steel shape on the seismic behaviour were analyzed. The results indicate that the configuration of these type shear walls was feasible. The seismic performance of composite concrete and steel plate shear walls with binding bars is well and the seismic performance is enhanced with different factors, such as the setting of end steel shape, the decreases of aspect ratio and binding bar spacing, the increases of plate thickness and core concrete thickness, etc.

KEYWORDS: *composite concrete and steel plate shear walls with binding bars; cyclic loading tests; seismic behavior.*

1. INSTRUCTIONS

The shear walls are one of the most critical elements in the high-rise or super high-rise structural system, which have long been used as an efficient lateral force-resisting system for building. With the increase of building height and the advance function requirement of architecture, the higher performance demand of structural walls were proposed. Steel plate -concrete composite walls are one of the new-style structural walls and have already been employed in the actual practice in recent years. It can be classified as steel plate reinforced concrete composite walls (SPRC) and concrete filled double steel plate (CFDSP) composite walls according to the different relative positions of the steel plates and concrete. Base on the interaction and cooperation of the two materials, the mechanical behavior of shear walls prominently changes.

Many researchers have carried out experimental and analytical studies on CFDSP walls in the past years, and several different configurations have been proposed. It was applied in the nuclear facilities, marine environment structures because of its superior behavior, large lateral stiffness, low cost and rapid construction. Wright et al. [1] conducted some pilot studies on the composite wall formed from two skins of profiled steel sheeting filled with concrete under different loading conditions and found that the steel sheeting provides similar characteristics to

conventional framework for concrete casting and finally to establish design formulas for actual practice [2–6] (Fig. 1.1a). Three 1/4 scale specimens of CFDSP walls with both horizontal and vertical diaphragms were built to take cyclic shear loading test by Emori K. [7] (Fig. 1.1b). The shear test exhibited high strength and significant ductility of these kinds of walls. Welded connection was used between the insert plates and the long-side steel plate, which would result in the deficiency of the steel plates and be difficult to be applied to the engineering. The Corus Company developed a CFDSP construction called Bi-Steel™ [8] with two surface steel plates connected by an array of transverse friction welded shear connectors (Fig. 1.1c), and a series of researches have been conducted on Bi-Steel [9–11]. In addition, Eom et al. [12] tested 5 isolated and 2 coupled CFDSP walls with rectangular and T-shaped cross sections under in-plane cyclic loading. The two surface steel plates of their test specimens were connected by tie bars, which was similar to Bi-Steel.

Considering the fact that the elements are hard to fabricate and may bring the residual stress in the steel plate when a large number of weld stud or panel is adopt, the composite concrete and steel plate shear walls with binding bars were proposed. In spite of extensive studies of CFDSP walls in the literature, the CFDSP walls with binding bars have not been fully addressed. In order to intensively investigate the seismic behavior of this new detailed concrete filled double-steel-plate composite wall, ten wall specimens were tested under axial compressive forces and reversed cyclic lateral loads. Failure mechanism, hysteric behavior, strength and deformation capacities, etc. are discussed in detail. The feasibility of the configuration was tested, and the influences of different factors on the behavior of shear walls were investigated.
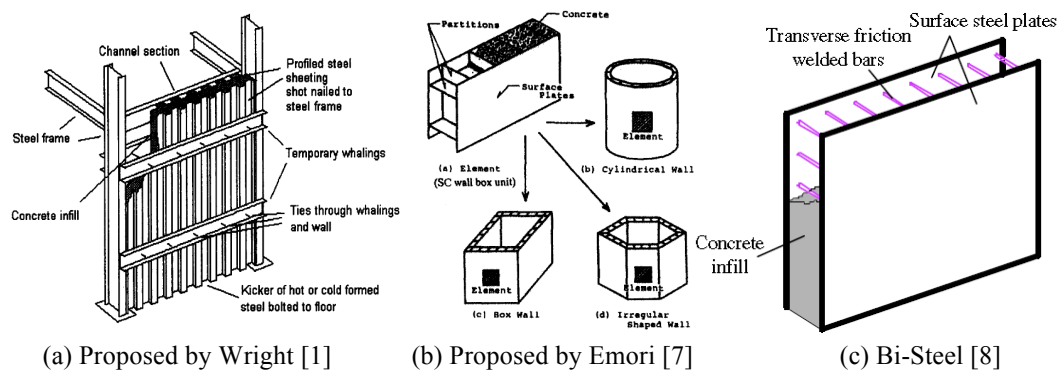

(a) Proposed by Wright [1]   (b) Proposed by Emori [7]   (c) Bi-Steel [8]

Figure 1.1 Previous developed CFDSP walls

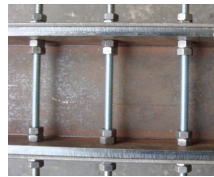## 2. EXPERIMENTAL PROGRAM

2.1. Test Specimens

Ten specimens with different parameters were designed and tested under high axial compressive forces and reversed cyclic lateral loads. The cross section and detailing of specimens are illustrated in Fig. 2.1.Two ends of the specimens (300mm deep) were embedded into the reinforced concrete basement and loading beam to simulate the boundary conditions of shear walls in buildings. The primary parameters were the aspect ratio, thickness of concrete wall, thickness of long-side steel plate, binding bar spacing, embedded section steel and axial compression ratio. The short-side steel plates of all the specimens are C section steel plates with thickness of 6mm.
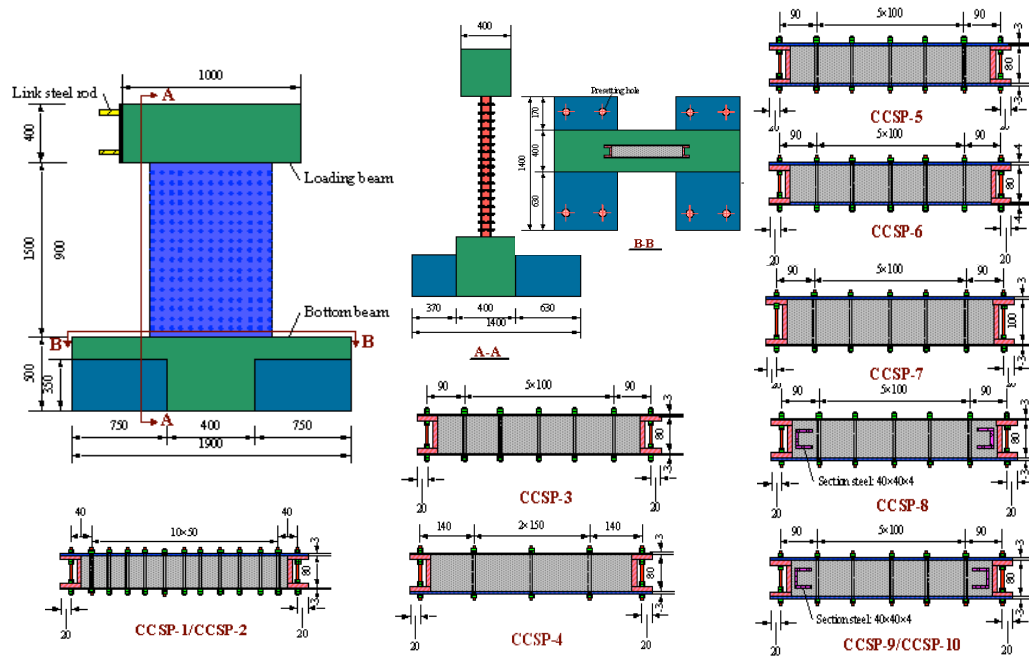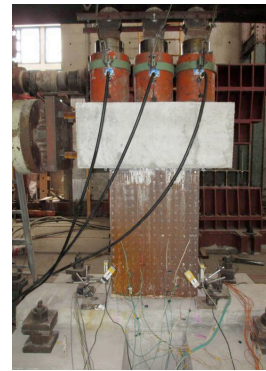
(a) Cross section

(b) Specimen construction (c) Bolt connection with eight nuts (d) Specimen installation

Figure 2.1 Detailing of Specimens of Composite concrete-steel plate shear walls with binding bars

Table 2.1. Tested specimens

Specimen	Dimension of cross section(mm) (width×depth)	Aspect ratio	Long-side plate thickness(mm)	Binding bar spacing (mm)	Embedded section steel	Axial compression ratio (n)
CCSP-1	620×86	1.5	3.0	50	No	0.4
CCSP -2	620×86	1.5	3.0	50	No	0.3
CCSP -3	620×86	1.5	3.0	100	No	0.3
CCSP -4	620×86	1.5	3.0	150	No	0.3
CCSP -5	620×86	2.5	3.0	100	No	0.3
CCSP -6	620×88	2.5	4.0	100	No	0.3
CCSP -7	620×106	2.5	3.0	100	No	0.3
CCSP -8	620×86	2.5	3.0	100	C40×40×4	0.3
CCSP -9	620×86	1.5	3.0	100	C40×40×4	0.3
CCSP-10	620×86	1.5	3.0	100	C40×40×4	0.4

2.2. Materials

All the walls were constructed with steel plates, binding bars and concrete. The average compressive strength (f_{cu}) of concrete was obtained by the test of nine cube samples (150×150×150mm), which gives f_{cu} =31.58MPa with a standard deviation of 1.19MPa. The measured properties of steel plates and binding bars are given in Table 2.2.

Table 2.2. Measured material properties

Type	Component	Yield stress(N/mm^2)	Ultimate stress(N/mm^2)
	3mm	321.7	465.6
Steel plate	4mm	259.8	371.7
	6mm	322.4	467.2
Binding bars	ø6	432.7	489.4

2.3. Test setup and loading procedure

The test setup is shown in Fig.2.2. The bottom beam was fixed to the reaction slab by eight screws. The axial compressive force N was first applied to the specimen by three vertical hydraulic jacks, which was maintained constant by a pressure gauge. N was calculated from Eq. (2.1) when n was given in Table 1. f_c is the compressive strength of concrete; f_y is the yield strength of steel plates; A_c and A_s are the cross-sectional areas of concrete and steel plates, respectively.

$$N=n\ (f_c A_c + f_y A_s) \qquad\qquad (2.1)$$

The lateral force was first controlled by load and then by top displacement. In the load control stage, the initial lateral load is set as 25 percent of the estimated yielding force. Before coming to the estimated yielding force, the applied load increases by a 20*kN* interval gradually at the beginning and a 10*kN* interval when close to the estimated yielding force. After exceeding the estimated yielding force, the loading scheme changes to a displacement controlled mode. For the specimens with aspect ratio of 1.5, the displacement of loading beam increases by 2mm in each loading step. For the specimens with aspect ratio of 2.5, the displacement of loading beam increases by 3mm in each loading step. Each loading step includes one complete cycle in the force-controlled phase and three cycles in the displacement-controlled phase. When the lateral force dropped below 85% of the maximum strength or the axial force could not be sustained, the test was stopped.

2.4. Instrumentation

All the specimens were instrumented to measure the loads, displacements and strains at critical locations. The arrangement of displacement meter is shown in Fig.2.3. Four displacement meters (LVDTs 1-4) were mounted to a rigid steel reference frame to measure lateral displacements, with the top one (LVDT 1) at the same height of the loading point. The diagonally of specimen arranged displacement meters were used to measure the shear deformations (LVDTs 5,6) and the bending deformation of the wall was measured by LVDTs 7,8. Steel strain gauges were arranged at different locations to measure the strain distribution of the specimens. Binding bars were chosen of each specimen to measure their stressing state.
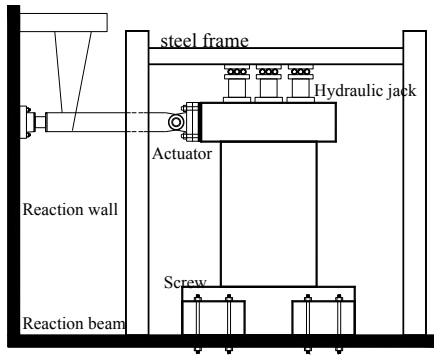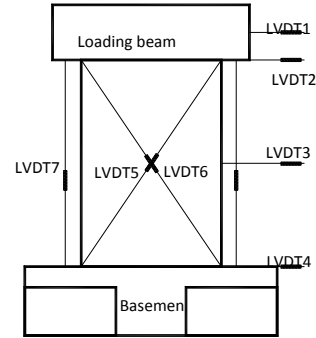
Figure 2.2 Test setup   Figure 2.3 Measuring points arrangement

3. EXPERIMENTAL RESULTS

3.1. Failure modes

The macroscopic damage occurred at the root of the wall in all specimens. Obvious local buckling, plastic deformation, out-plane instability, fracture and the crack of the concrete were observed. Take specimen CCSP-1 as the example, the failure mode is shown in Fig. 3.1. The loading process could be divided into three stages: pre-yielding stage (from beginning to yielding point on the load-displacement envelope curve), plastic stage (from yielding point to the peak point) and failure stage. Six specimens with shear span ratio of 1.5 showed the shearing-dominated behaviour and four specimens with shear span ratio 2.5 showed flexure behaviour.

For all specimens, the local buckling took place in the bolt connection area of the long-side steel plate in the root on the edge, some specimens even developed fracture. In the initiation of local buckling, the lateral force was already close to the maximum strength, and at the maximum strength, the local buckling hadn't developed obviously. Therefore, the fracture of the plate where occurred local buckling might not significantly affect the loading-carry capacities of the specimens, for the loading-carry capacities of the specimens had nearly fully developed before the initiation of fracture. However, the fracture propagation caused the final loss of loading-carry capacities, which might affect the deformation capacities of the specimens.
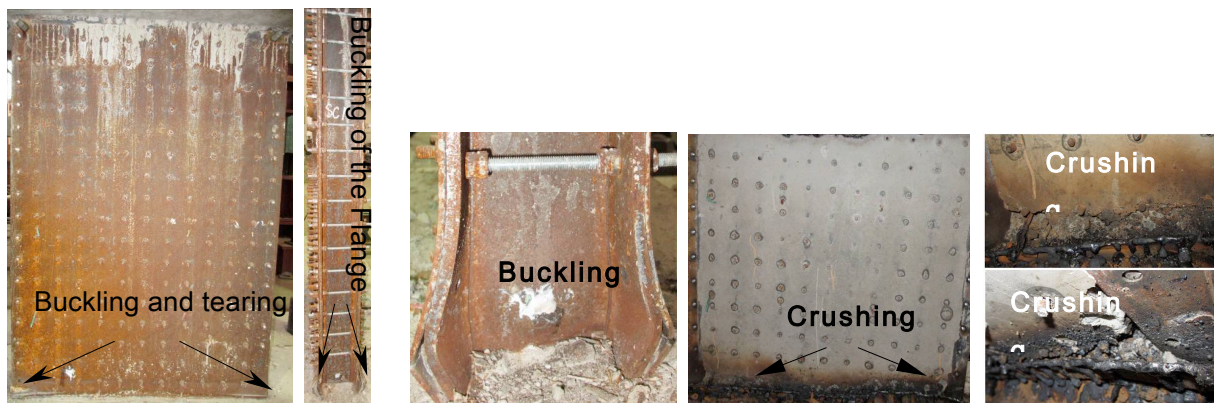

Figure 3.1 Failure mode of specimen CCSP-1

The test results and the failure modes for all specimens are illustrated in Table 3.1. As we can see from the data, increases of the thickness of steel plate or concrete, embedment of channel steel, decreasing the spacing of binding bars can improve the bearing capacity of specimen. Increase the axial compression ration can reduce the

bearing capacity when the value of n is high. And decreasing the spacing of binding bars can prominently improve the mechanical stability of shear walls.

Table 3.1 The typical values of lateral force and displacement

NO.	Yielding state		Peak state		Failure state		Ductility	Failure mode
	$V_y(KN)$	$\theta_y(rad)$	$V_u(KN)$	$\theta_u(rad)$	$V_d(KN)$	$\theta_d(rad)$	$\mu=\theta_d/\theta_y$	
CCSP-1	+322.6	+1/176	+377.9	+1/76	+321.5	+1/41	+4.21	CBL,BS,TL
	-300.5	-1/189	-358.9	-1/68	-305.1	-1/41	-4.61	CC,FB
CCSP-2	+318.5	+1/131	+383.1	+1/64	+325.6	+1/36	+3.65	CBL,BS,TL
	-307.6	-1/134	-364.9	-1/56	-309.3	-1/34	-3.89	TS,CC,FB
CCSP-3	+306.8	+1/162	+372.0	+1/80	+316.2	+1/56	+2.87	CBL,BS,
	-271.9	-1/170	-325.7	-1/68	-276.8	-1/54	-3.17	CC,FB
CCSP-4	+253.2	+1/206	+305.5	+1/105	+259.7	+1/69	+2.99	CBL,CC
	-239.0	-1/192	-293.5	-1/90	-267.1	-1/66	-2.92	DC,FB
CCSP-5	+196.8	+1/161	+235.3	+1/103	+200.0	+1/62	+2.61	CBL,CC
	-172.3	-1/174	-208.0	-1/82	-176.8	1/60	-2.89	BS,FB
CCSP-6	+227.7	+1/140	+271.7	+1/73	+230.9	+1/52	+2.69	CBL,CC
	-213.3	-1/136	-257.6	-1/71	-219.0	-1/51	-2.65	BS,FB
CCSP-7	+202.3	+1/154	+248.1	+1/80	+210.9	+1/46	+3.37	CBL,CC
	-194.7	-1/161	-235.4	-1/74	-200.0	-1/46	-3.52	BS,FB
CCSP-8	+225.1	+1/182	+259.6	+1/93	+220.7	+1/59	+3.08	CBL,CC
	-203.1	-1/202	-243.3	-1/91	-224.2	-1/50	-4.03	BS,FB
CCSP-9	+364.4	+1/135	+420.0	+1/76	+357.0	+1/46	+2.96	CBL,BS,DC
	-309.8	-1/163	-393.1	-1/79	-334.1	-1/51	-3.22	CC,FB,BES
CCSP-10	+329.7	+1/179	+403.8	+1/93	+343.2	+1/63	+2.84	CBL,BS,DC
	-301.6	-1/194	-381.3	-1/90	-324.1	-1/63	-3.06	CC,FB,BES

Note: "+" presents the positive loading direction; "-" presents the negative loading direction; CBL=convex buckling of long-side steel plate; BS= buckling of short-side steel plate; TL=tearing of long-side steel plate; TS=tearing of short-side steel plate; CC=crushing of concrete; DC=diagonal cracks of concrete; FB= fracture of bolt connection; BES=buckling of embedded section steel

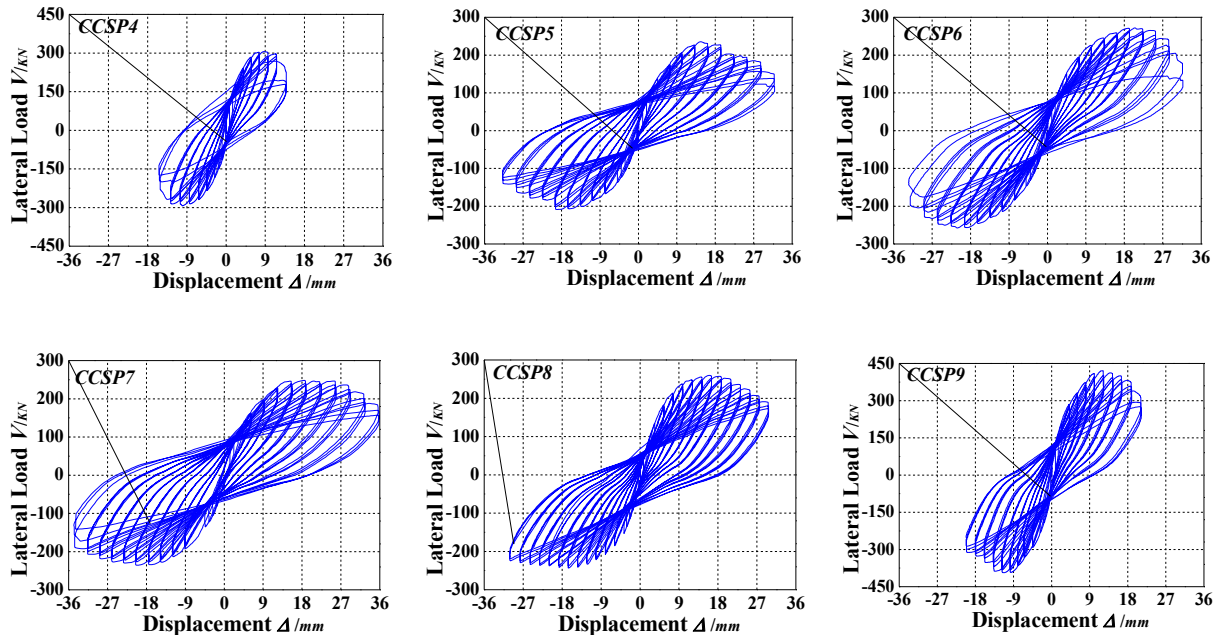## 3.2. Lateral force versus top displacement curves
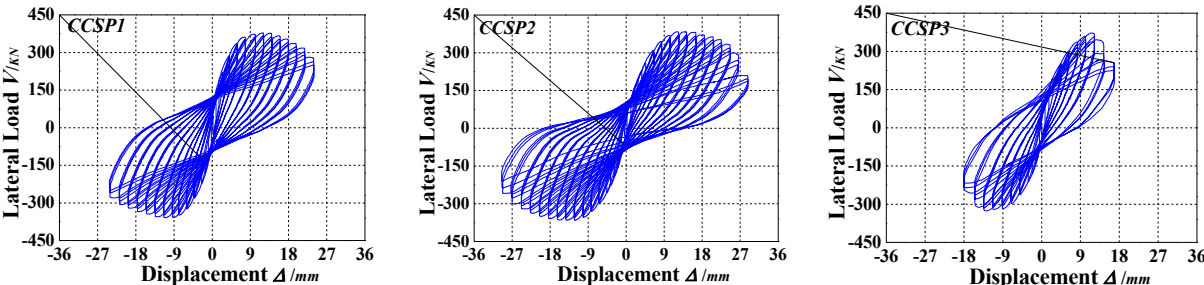
Figure 3.2 Lateral force versus top displacement curves of specimens

The envelope curve was obtained from these hysteretic response curves which are shown in Fig.3.2. The specimens' envelope curves for the first loading cycle are presented in Fig.3.3. From the comparison of the experimental results, we can conclude that the specimen with larger axial-load ratio, or setting of end steel shape, or decreasing the spacing of binding bars, or increasing the thickness of steel plate, or increasing the aspect ratio can effectively enhance the energy dissipation capacity of the specimen.

3.3.Energy dissipation

As shown in Fig. 3.4, the accumulated energy dissipation during the first cycle at each displacement was calculated quantitatively based on the hysteretic response curves. Compared to the different specimens, the specimens which were embedded channel steel at the end of sections or shorten the spacing of binding bars show a significant increase of energy dissipation capacity.
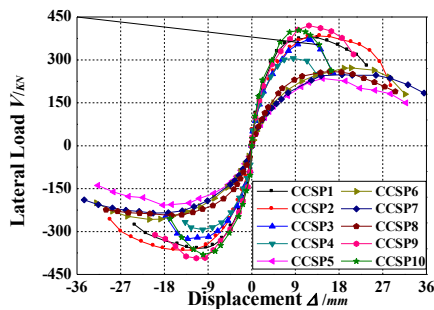

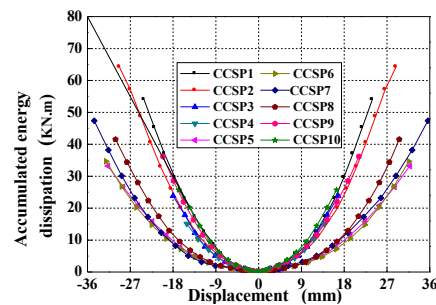Figure 3.3 The envelope curves of specimens

Figure 3.4 Accumulated energy dissipation curves

4. CONCLUSIONS

In this paper the seismic behavior of ten specimens of concrete filled double steel plate (CFDSP) composite walls with binding bars were experimentally studied under axial compressive forces and reversed cyclic lateral loads. The proposed CFDSP wall exhibited good seismic behavior in the tests and could provide a favorable choice for the specific structural demand. The main conclusions drawn in this research can be summarized as follows:

(1) The CFDSP walls with binding bars exhibit excellent performance in bearing capacity, ductility, energy dissipation, lateral stiffness and smart system. It is a kind of composite elements of steel and concrete with outstanding seismic behavior.

(2) The configuration of CFDSP walls with binding bars is feasible. The bolt connection can effectively restrict the elements and improved the ductility.

(3) The decrease of spacing of binding bars has an significant effect on the ductility and the shear capacity.

(4) Increasing the thickness of steel plate or concrete, embedment of channel steel can improve the bearing capacity and ductility of specimen. And setting of end steel shape can improve prominently.

REFERENCES

1. Wright HD, Gallocher SC (1995). The behavior of composite walling under construction and service loading. J Constr Steel Res. **35:3**, 57–273.
2. Wright HD, Hossain K (1997). In-plane shear behavior of profiled steel sheeting. Thin Walled Struct .**29:1–4**, 79–100.
3. Wright H (1998). The axial load behavior of composite walling. J Constr Steel Res. 45(3):353–375.
4. Hossain K, Wright HD (1998). Performance of profiled concrete shear panels. J Struct Eng ASCE.**124:4**, 368-381.
5. Hossain K, Wright HD (2004). Experimental and theoretical behavior of composite walling under in-plane shear. J Constr Steel Res.**60:1**, 59–83.
6. Hossain K, Wright HD (2004). Performance of double skin-profiled composite shear walls —experiments and design equations. Can J Civ Eng .**31:2**, 204–217.
7. Emori K (2002). Compressive and shear strength of concrete filled steel box wall. Steel Structures.**68:2**, 29~40.
8. Bowerman HG, Gough MS, King CM (1999). Bi-Steel design and construction guide. British Steel Ltd..
9. Clubley SK, Moy S, Xiao RY (2003). Shear strength of steel–concrete–steel composite panels. Part I—testing and numerical modelling. J Constr Steel Res.**59:6**, 781–794.
10. Clubley SK, Moy S, Xiao RY (2003). Shear strength of steel–concrete–steel composite panels. Part II—detailed numerical modelling of performance. J Constr Steel Res .59(6):795–808.
11. Xie M, Chapman JC (2006). Developments in sandwich construction. J Constr Steel Res .**62:11SI**, 1123–1133.
12. Eom TS, Park HG, Lee CH, Kim JH, Chang IH (2009). Behavior of double skin composite wall subjected to in-plane cyclic loading. J Struct Eng ASCE.**135:10**, 1239–1249.